Proceedings of the Canadian Society for Mechanical Engineering International Congress 2022
CSME Congress 2022
June 5-8, 2022, Edmonton, AB, Canada

Developing a Dynamic Model of the Standard Neonatal Patient Transport System using Lagrange's Equation in the Pitch Plane

K. Gibb[1], P. Kehoe[1], J. Hurley[1], C. Aubertin[2], K. Greenwood[2], A. Ibey[2,3], S. Redpath[2], A.D.C. Chan[3], J.R. Green[3], R.G. Langlois[1]
[1]Mechanical and Aerospace Engineering, Carleton University, Ottawa, Canada
[2] Children's Hospital of Eastern Ontario, Ottawa, Ontario, Canada
[3] Systems and Computer Engineering, Carleton University, Ottawa, Canada

Abstract— During transport to critical care centres, neonatal patients can be exposed to elevated levels of vibration which may pose a risk to the patients' health. In Ontario, a standardized Neonatal Patient Transport System (NPTS) has been implemented in ground and air ambulances, and studies to characterize the vibration environment within these vehicles are underway. The development of a dynamic model of the NPTS is intended to support the study of emergency vehicle vibration environments and strategies to mitigate vibration amplification. This paper outlines the derivations of equations of motion for a planar model of the NPTS. This derivation uses the Lagrangian approach to develop equations governing motion in the pitch plane. Stiffness and damping coefficients were optimized to drive the frequency response of the developed dynamic model towards data recorded during on-road testing. Future development of the model will involve deriving the equations for the roll plane, and further optimization of stiffness and damping parameters to ensure they adequately represent the response for various transport conditions.

Keywords – neonatal transport, vibration analysis, frequency response, dynamic model, power spectral density

I. INTRODUCTION

Neonatal patients require specialized care during interfacility transport by ground and air ambulance. A standardized neonatal transport incubator has been introduced in Ontario to ensure interoperability of equipment across different medical institutions and emergency vehicles [1]. Despite this Neonatal Patient Transport System (NPTS) providing necessary medical support to the patient in transport, there are concerns regarding whole-body vibrations to which neonates are exposed, particularly in the vertical direction.

Physical stressors such as whole-body vibration or shock may have a detrimental effect on the patient in transport. Long-term high-intensity whole-body vibration is identified as a health risk by the International Organization for Standardization [2]. Neonates are particularly vulnerable, which motivates vibration mitigation within the NPTS. This research is a part of a collaborative project between Carleton University, the Children's Hospital of Eastern Ontario (CHEO), and other industry and government partners to identify the sources of, and ultimately reduce, the vibrations to which neonates are subjected during emergency transport. Studies are underway to characterize the vibration environment of emergency vehicles, identify sources of amplification, and test various mitigation strategies. The initial stages of testing involve data capture within the emergency vehicle, followed by parametric studies performed in the laboratory. Coordinating availability of vehicles and equipment, as well as conducting and processing data is time consuming and costly. A dynamic model is being developed to assist in studying the system dynamics, without the need to remove the NPTS and ambulance from service for testing. The intention of the model is to reproduce the frequency response of the NPTS, such that it may be used as a predictive tool for various transport environments or vibration mitigation approaches. The first stages of developing this model include deriving the equations of motion about the roll and pitch planes to identify unknown parameters in the more complex model. The equations in the pitch plane were derived by applying Lagrange's equation, and the model parameters were then tuned to drive the acceleration power spectral density (PSD) predicted by the model towards the response recorded during testing in a ground ambulance.

In recent years, modelling of vehicle dynamics for the purpose of stretcher parameter optimization has been performed by Yang et al. to study vibration attenuation within tracked ambulances [3], and by Malvezzi et al. by using the Lagrange formulation to develop an 8-DOF vehicle and stretcher model [4]. Transport systems have also been modelled for the purpose of vibration isolation using passive and semi-active control solutions, such as by Chae and Choi's magnetorheological dampers model [5], and Bailey-Van Kuren and Shukla's air springs models [6].

The purpose of this paper is to detail the development of a planar model and evaluate the simulated motion by comparing against data recorded during on-road testing. This model is to be used for parameter identification, but will be extended in future studies to aid in vibration mitigation.

II. Neonatal Patient Transport System

The NPTS refers to the medical equipment configured on top of a stretcher, including the incubator in which the patient is harnessed atop a mattress. The equipment is in a stacked configuration, secured to a deck which mechanically interfaces with the stretcher frame using clamps.

This dynamic model is designed to replicate the data recorded during preliminary on-road ambulance testing. This testing included various road types and the collected data were used to provide the representative random input for in-laboratory shaker tests [7]. Inertial measurement unit (IMU) data recorded at the floor of the vehicle provided input motion for the dynamic model, while the vertical motion at the centre of mass of the stretcher and the chest of the baby manikin were compared to the simulation. The segment of on-road testing that was replicated by the MATLAB simulation is along a high-speed arterial road, recorded over a duration of 278 seconds.

III. Dynamic Model

This planar model is the first stage in developing a three-dimensional, seven-degree-of-freedom multi-body dynamic model of the NPTS. The purpose of deriving equations for the roll and pitch planes is to identify system parameters that are to be implemented in the more complex model. This is done by tuning the planar model to replicate the vertical acceleration PSD experienced in the physical system.

The model assumes rigid fixtures between the stretcher, deck, and incubator, such that these components could be considered as a single rigid body. The entire system, including the stretcher, will be referred to as the NPTS for simplicity. Three linear spring-dampers are used: two to model the interface between the NPTS and the vehicle floor, and one to represent the viscoelastic properties of the mattress. The orientation of the NPTS is that which is used in a ground ambulance by the Ottawa Paramedic Service, where the stretcher is positioned longitudinally along the vehicle, slightly offset to the left of the vehicle centreline, with the foot of the stretcher pointed towards the rear and the incubator facing the front.

A. Pitch Model

Following the standard SAE vehicle coordinate system, the pitch model represents the NPTS as viewed from the side, with pitch occurring about the vehicle's lateral axis [8]. The diagram presented in Fig. 1 depicts the geometry of the system. The centre of mass is approximated by the relative weights of medical equipment included in the NPTS, with the mass of the patient offset to indicate the incubator position. The patient mass, m, is treated as a point mass. Given the loading mechanism secures to the head of the stretcher, the equivalent stiffness and damping representing the wheel pairs at the foot and head of the stretcher cannot be assumed equal. Dimensions and mass properties are shown in Table I [9,10]. The input motion applied to the vehicle floor has three components: heave (z), surge (x), and pitch (θ).

TABLE I. Pitch Model Properties

Model Properties		
Parameter	***Symbol***	***Value***
Initial height of patient from datum	h	0.6 m
Initial height of NPTS centre of mass from datum	r	0.43 m
Distance from centre of mass to foot of stretcher	d_1	0.99 m
Distance from centre of mass to head of stretcher	d_2	1.04 m
Forward offset of patient from NPTS centre of mass	f	0.335 m
Mass of NPTS and stretcher	M	227.5 kg
Mass moment of inertia about the NPTS centre of mass	I_y	72.8 kgm^2
Mass of patient	m	2.5 kg

The pitch model is considered first, as the model geometry may be simplified to provide the roll model equations. Future work includes developing the roll model and evaluating the frequency response in the roll plane.

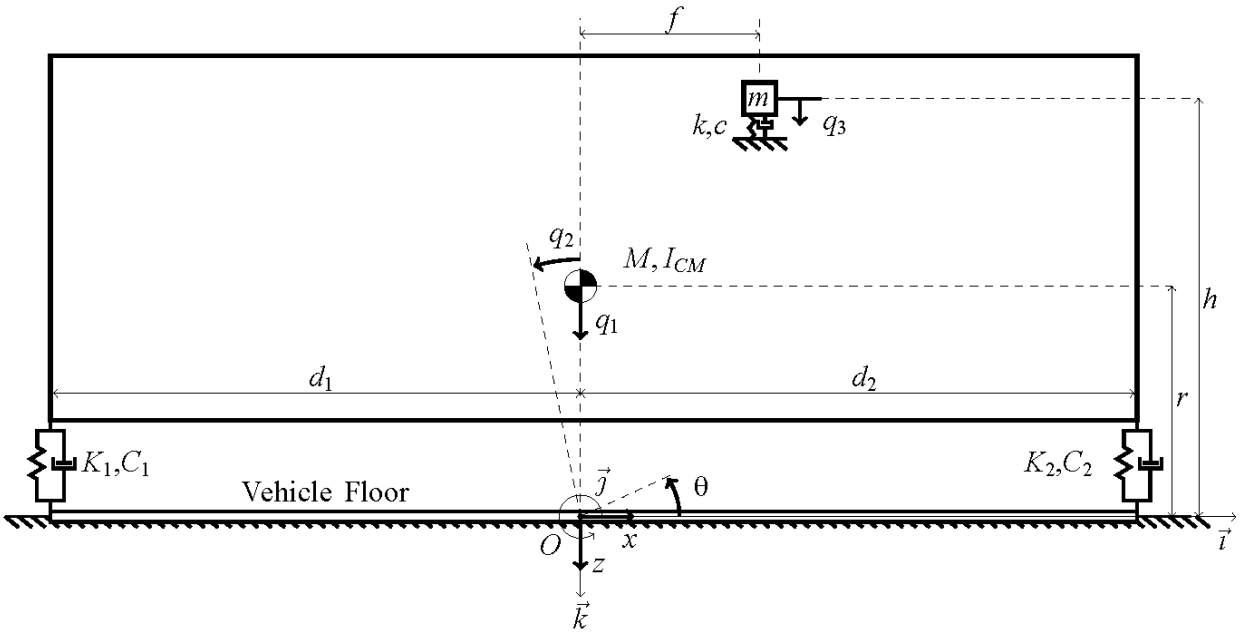

Figure 1. Diagram of planar dynamic model in the pitch plane.

IV. Equations of Motion

The planar dynamic model is a three-degree-of-freedom problem with three generalized coordinates: q_1 represents the displacement of the NPTS along its vertical axis; q_2 is the angular position of the NPTS; and q_3 is the vertical displacement of the baby mass located within the incubator, measured relative to its initial position on the NPTS. Coordinate q_2 is measured relative to the vehicle floor; it is assumed that the NPTS pitches purely about the pivot point on the floor, due to the constraint imposed by the floor interface.

The vehicle floor is initially aligned with, and moves relative to, the global coordinates fixed at Point *O*. The absolute positions of masses *M* and *m* must account for their relative positions with respect to the floor.

A. Kinematics

$$\vec{p}_M = (q_1 - r)\sin q_2\,\vec{i} + (q_1 - r)\cos q_2\,\vec{k} \tag{1}$$

and

$$\begin{aligned}\vec{p}_m = &\left((q_1 + q_3 - h)\sin q_2 + f\cos q_2\right)\vec{i} \\ &+ \left((q_1 + q_3 - h)\cos q_2 - f\sin q_2\right)\vec{k}.\end{aligned} \tag{2}$$

Taking the first derivate with respect to time,

$$\begin{aligned}\vec{v}_M = &(\dot{q}_1\sin q_2 + (q_1 - r)\dot{q}_2\cos q_2)\vec{i} \\ &+ (\dot{q}_1\cos q_2 - (q_1 - r)\dot{q}_2\sin q_2)\vec{k}\end{aligned} \tag{3}$$

and

$$\begin{aligned}\vec{v}_m = &\left((\dot{q}_1 - f\dot{q}_2 + \dot{q}_3)\sin q_2 + (q_1 + q_3 - h)\dot{q}_2\cos q_2\right)\vec{i} \\ &+ \left((\dot{q}_1 - f\dot{q}_2 + \dot{q}_3)\cos q_2 - (q_1 + q_3 - h)\dot{q}_2\sin q_2\right)\vec{k}.\end{aligned} \tag{4}$$

B. Lagrange's Equation

The equations of motion were determined by using the Lagrange method, which must satisfy

$$\frac{d}{dt}\left(\frac{\partial L}{\partial \dot{q}_r}\right) - \frac{\partial L}{\partial q_r} = Q_{q_r} \tag{5}$$

for each of the generalized coordinates, *r*. Generalized forces are represented by Q_{q_r}, and *L*, the Lagrangian, is equal to

$$L = T - U \tag{6}$$

where *T* is the kinetic energy of the system and *U* is the potential energy.

The kinetic energy is expressed by

$$T = \sum_{bodies}\left(\tfrac{1}{2}mv^2 + \tfrac{1}{2}I\omega^2\right) \tag{7}$$

Considering both bodies, this becomes

$$T = \tfrac{1}{2}Mv_M^2 + \tfrac{1}{2}I_y\omega_y^2 + \tfrac{1}{2}mv_m^2. \tag{8}$$

The angular velocity ω_y of the NPTS can be expressed by the generalized coordinates. Given $\omega_y = \frac{v_x}{r}$, the velocity of the NPTS is rotated from the global reference frame to a local reference frame aligned with the NPTS body

$$\vec{v}_{M_{local}} = \mathbf{R}\vec{v}_{M_{global}} \tag{9}$$

where

$$\mathbf{R} = \begin{bmatrix}\cos q_2 & 0 & -\sin q_2 \\ 0 & 1 & 0 \\ \sin q_2 & 0 & \cos q_2\end{bmatrix}. \tag{10}$$

This gives

$$\vec{v}_{M_{local}} = (q_1 - r)\dot{q}_2\vec{i} + \dot{q}_1\vec{k} \tag{11}$$

and the angular velocity ω_y is found to be

$$\omega_y = \frac{(q_1 - r)\dot{q}_2}{(q_1 - r)} = \dot{q}_2. \tag{12}$$

The squared velocities of each body in the global reference frame are,

$$v_M^2 = v_M \cdot v_M = \dot{q}_1^2 + (q_1 - r)^2\dot{q}_2^2 \tag{13}$$

$$v_m^2 = v_m \cdot v_m = (\dot{q}_1 - f\dot{q}_2 + \dot{q}_3)^2 + (q_1 + q_3 - h)^2\dot{q}_2^2. \tag{14}$$

Equation (8) now becomes

$$\begin{aligned}T = &\tfrac{1}{2}M\left(\dot{q}_1^2 + (q_1 - r)^2\dot{q}_2^2\right) + \tfrac{1}{2}I_y\dot{q}_2^2 \\ &+ \tfrac{1}{2}m\left((\dot{q}_1 - f\dot{q}_2 + \dot{q}_3)^2 + (q_1 + q_3 - h)^2\dot{q}_2^2\right).\end{aligned} \tag{15}$$

The potential energy due to spring stiffness can be found. It is assumed that the spring-dampers are constrained to act vertically, such that small angle approximations may be made with regard to q_2, leading to

$$\begin{aligned}U = &\tfrac{1}{2}K_1(q_1 + d_1q_2 - z - d_1\sin\theta)^2 \\ &+ \tfrac{1}{2}K_2(q_1 - d_2q_2 - z + d_2\sin\theta)^2 + \tfrac{1}{2}kq_3{}^2\end{aligned} \tag{16}$$

Substituting (15) and (16) in (6), the Lagrangian is found to be

$$\begin{aligned}L = &\tfrac{1}{2}M\left(\dot{q}_1^2 + (q_1 - r)^2\dot{q}_2^2\right) + \tfrac{1}{2}I_yq_2^2 \\ &+ \tfrac{1}{2}m\left((\dot{q}_1 - f\dot{q}_2 + \dot{q}_3)^2 + (q_1 + q_3 - h)^2\dot{q}_2^2\right) - \tfrac{1}{2}kq_3{}^2 \\ &- \tfrac{1}{2}K_1(q_1 + d_1q_2 - z - d_1\sin\theta)^2 - \tfrac{1}{2}K_2(q_1 - d_2q_2 - z + d_2\sin\theta)^2\end{aligned} \tag{17}$$

and the partial derivatives of each generalized coordinate required in (5) are found to be

$$\frac{\partial L}{\partial q_1} = M(q_1 - r)\dot{q}_2^2 + m(q_1 + q_3 - h)\dot{q}_2^2 - K_1(q_1 + d_1 q_2 - z - d_1 \sin\theta) - K_2(q_1 - d_2 q_2 - z + d_2 \sin\theta) \tag{18}$$

$$\frac{\partial L}{\partial \dot{q}_1} = M\dot{q}_1 + m(\dot{q}_1 - f\dot{q}_2 + \dot{q}_3) \tag{19}$$

$$\frac{\mathrm{d}}{\mathrm{dt}}\left(\frac{\partial L}{\partial \dot{q}_1}\right) = M\ddot{q}_1 + m(\ddot{q}_1 - f\ddot{q}_2 + \ddot{q}_3) \tag{20}$$

$$\frac{\partial L}{\partial q_2} = -K_1 d_1(q_1 + dq_2 - z - d_1 \sin\theta) + K_2 d_2(q_1 - dq_2 - z + d_2 \sin\theta) \tag{21}$$

$$\frac{\partial L}{\partial \dot{q}_2} = M(q_1 - r)^2\dot{q}_2 - fm(\dot{q}_1 - f\dot{q}_2 + \dot{q}_3) + m(q_1 + q_3 - h)^2\dot{q}_2 + I_y\dot{q}_2 \tag{22}$$

$$\frac{\mathrm{d}}{\mathrm{dt}}\left(\frac{\partial L}{\partial \dot{q}_2}\right) = 2M(q_1 - r)\dot{q}_1\dot{q}_2 + M(q_1 - r)^2\ddot{q}_2 - fm(\ddot{q}_1 - f\ddot{q}_2 + \ddot{q}_3) + 2m(q_1 + q_3 - h)(\dot{q}_1 + \dot{q}_3)\dot{q}_2 + m(q_1 + q_3 - h)^2\ddot{q}_2 + I_y\ddot{q}_2 \tag{23}$$

$$\frac{\partial L}{\partial q_3} = m(q_1 + q_3 - h)\dot{q}_2^2 - kq_3 \tag{24}$$

$$\frac{\partial L}{\partial \dot{q}_3} = m(\dot{q}_1 - f\dot{q}_2 + \dot{q}_3) \tag{25}$$

$$\frac{\mathrm{d}}{\mathrm{dt}}\left(\frac{\partial L}{\partial \dot{q}_3}\right) = m(\ddot{q}_1 - f\ddot{q}_2 + \ddot{q}_3). \tag{26}$$

The damping forces, weights of the two masses, and applied floor force are considered generalized forces. These forces are found using

$$Q_{q_r} = \vec{F} \cdot \frac{\partial \vec{p}_F}{\partial \vec{q}_r}. \tag{27}$$

Due to use of the dot product in (28), a force vector acting in a single direction will only be scaled by the position component in the same direction. Let $\vec{F}_{sp_1}$ be the damping force on the bottom left spring-damper, $\vec{F}_{sp_2}$ be the damping force of the bottom right spring-damper, $\vec{F}_{sp_3}$ be the force due to the mattress damping on M, $\vec{F}_{sp_4}$ be the force due to the mattress damping on m, and $\vec{W}_{\mathrm{M}}$ and $\vec{W}_{\mathrm{m}}$ be the weights of the two masses. $\vec{F}_{\mathrm{y}}$ is the lateral force due to movement of the ambulance floor, and is assumed to be applied at the floor level directly under the NPTS centre of mass. These forces, positions, and derivatives of position, after small angle approximation, with respect to each generalized coordinate are given in Table II. Applying (28) to q_1, q_2, and q_3 gives

$$Q_{q_1} = -C_1(\dot{q}_1 + d_1\dot{q}_2 - \dot{z} - d_1\dot{\theta}\cos\theta) - C_2(\dot{q}_1 - d_2\dot{q}_2 - \dot{z} + d_2\dot{\theta}\cos\theta) + c\dot{q}_3 - c\dot{q}_3 + Mg + mg + \frac{I_y\ddot{x}}{(r + z - q_1)^2}q_2 - \frac{I_y\ddot{x}}{(r + z - q_1)^2}q_2 \tag{28}$$

$$Q_{q_2} = -C_1 d_1(\dot{q}_1 + d_1\dot{q}_2 - \dot{z} - d_1\dot{\theta}\cos\theta) + C_2 d_2(\dot{q}_1 - d_2\dot{q}_2 - \dot{z} + d_2\dot{\theta}\cos\theta) - cf\dot{q}_3 + cf\dot{q}_3 - mgf + \frac{I_y\ddot{x}}{(r + z - q_1)} \tag{29}$$

and

$$Q_{q_3} = -c\dot{q}_3 + mg. \tag{30}$$

Equations (18), (20), (21), (23), (24), (26) and (28)-(30) were then applied to (5) in order to find the equations of motion. The equations have been verified by comparing them against those derived independently using the Newton-Euler approach, the process of which is to be presented in a future paper.

The resulting equations of motion can be presented in matrix form, as shown in Eq. (31).

TABLE II. GENERALIZED FORCE COMPONENTS

Vertical Force	**Force and Position Components**				
	Component $(\vec{k})$	***Position before small angle approximation*** $(\vec{k})$	$\frac{\partial \boldsymbol{p}}{\partial \boldsymbol{q_1}}(\vec{k})$	$\frac{\partial \boldsymbol{p}}{\partial \boldsymbol{q_2}}(\vec{k})$	$\frac{\partial \boldsymbol{p}}{\partial \boldsymbol{q_3}}(\vec{k})$
$\vec{F}_{sp_1}$	$-C_1(\dot{q}_1 + d_1\dot{q}_2 - \dot{z} - d_1\dot{\theta}\cos\theta)$	$-(h_{1/O} + z - q_1)\cos q_2 + d_1 \sin q_2$	1	d_1	0
$\vec{F}_{sp_2}$	$-C_2(\dot{q}_1 - d_2\dot{q}_2 - \dot{z} + d_2\dot{\theta}\cos\theta)$	$-(h_{1/O} + z - q_1)\cos q_2 - d_2 \sin q_2$	1	$-d_2$	0
$\vec{F}_{sp_3}$	$c\dot{q}_3 \cos q_2$	$-(h + z - q_1)\cos q_2 - f\sin q_2$	1	$-f$	0
$\vec{F}_{sp_4}$	$-c\dot{q}_3 \cos q_2$	$-(h + z - q_1 - q_3)\cos q_2 - f\sin q_2$	1	$-f$	1
$\vec{W}_M$	Mg	$-(r + z - q_1)\cos q_2$	1	0	0
$\vec{W}_m$	mg	$-(h + z - q_1 - q_3)\cos q_2 - f\sin q_2$	1	$-f$	1
$\vec{F}_x$	$\frac{I_y\ddot{x}}{(r + z - q_1)^2}\sin q_2$	$-(r + z - q_1)\cos q_2$	1	0	0
Lateral Force	***Component*** $(\vec{i})$	***Position before small angle approximation*** $(\vec{i})$	$\frac{\partial \boldsymbol{p}}{\partial \boldsymbol{q_1}}(\vec{i})$	$\frac{\partial \boldsymbol{p}}{\partial \boldsymbol{q_2}}(\vec{i})$	$\frac{\partial \boldsymbol{p}}{\partial \boldsymbol{q_3}}(\vec{i})$
$\vec{F}_x$	$\frac{I_y\ddot{x}}{(r + z - q_1)^2}\cos q_2$	$(r + z - q_1)\sin q_2$	$-q_2$	$r + z - q_1$	0

$$\begin{bmatrix} M+m & -fm & m \\ -fm & Mr^2+m\left(f^2+h^2\right)+I_y & -fm \\ m & -fm & m \end{bmatrix}\begin{Bmatrix} \ddot{q}_1 \\ \ddot{q}_2 \\ \ddot{q}_3 \end{Bmatrix}+\begin{bmatrix} C_1+C_2 & C_1d_1-C_2d_2 & 0 \\ C_1d_1-C_2d_2 & C_1d_1^2+C_2d_2^2 & 0 \\ 0 & 0 & c \end{bmatrix}\begin{Bmatrix} \dot{q}_1 \\ \dot{q}_2 \\ \dot{q}_3 \end{Bmatrix}+\begin{bmatrix} K_1+K_2 & K_1d_1-K_2d_2 & 0 \\ K_1d_1-K_2d_2 & K_1d_1^2+K_2d_2^2 & 0 \\ 0 & 0 & k \end{bmatrix}\begin{Bmatrix} q_1 \\ q_2 \\ q_3 \end{Bmatrix}$$

$$=\begin{Bmatrix} M\dot{q}_2^2\left(q_1-r\right)+m\dot{q}_2^2\left(q_1+q_3-h\right)+C_1\left(\dot{z}+d_1\dot{\theta}\cos\theta\right)+C_2\left(\dot{z}-d_2\dot{\theta}\cos\theta\right)+K_1\left(z+d_1\sin\theta\right)+K_2\left(z-d_2\sin\theta\right)+Mg+mg \\ -2M\left(\dot{q}_1\dot{q}_2\left(q_1-r\right)+\ddot{q}_2\left(q_1^2-2q_1r\right)\right)-m\left(2\dot{q}_2\left(q_1+q_3-h\right)\left(\dot{q}_1+\dot{q}_3\right)+\ddot{q}_2\left(q_1^2+2q_1q_3+q_3^2-2hq_1-2hq_3\right)\right) \\ +C_1d_1\left(\dot{z}+d_1\dot{\theta}\cos\theta\right)+C_2d_2\left(-\dot{z}+d_2\dot{\theta}\cos\theta\right)+K_1d_1\left(z+d_1\sin\theta\right)+K_2d_2\left(-z+d_2\sin\theta\right)-fmg+\dfrac{I_y\ddot{x}}{\left(r+z-q_1\right)} \\ m\left(q_1+q_3-h\right)\dot{q}_2^2+mg \end{Bmatrix} \tag{31}$$

V. Results

A random vibration input was used to provide the floor motion in the *z*, *x*, and θ directions, and the equations of motion were used to simulate the system response in MATLAB. Random motion was generated using data from the floor accelerometer and IMU, recorded during road testing. Fig. 2 illustrates the input motion, and Figs. 3–5 present the simulated vertical displacement and acceleration of the NPTS and neonate, and angular acceleration of the NPTS. Solving for the eigenvalues of the equations, the natural frequencies were found to be 7.93 Hz, 9.26 Hz, and 12.41 Hz, and the damped natural frequencies were 7.82 Hz, 9.05 Hz and 12.20 Hz.

The acceleration spectral densities were found using Welch's power spectral density estimate, using data segmentation windows having 1000 points with 50% overlap. Figs. 6–8 present the PSDs from the road test data and dynamic model simulation. The stiffness and damping coefficients were manually tuned to drive the peak values of the vertical PSDs toward the objective values and reduce the root-mean-square error between the curves. The parameters representing the equivalent stiffness and damping across the NPTS are presented in Table III.

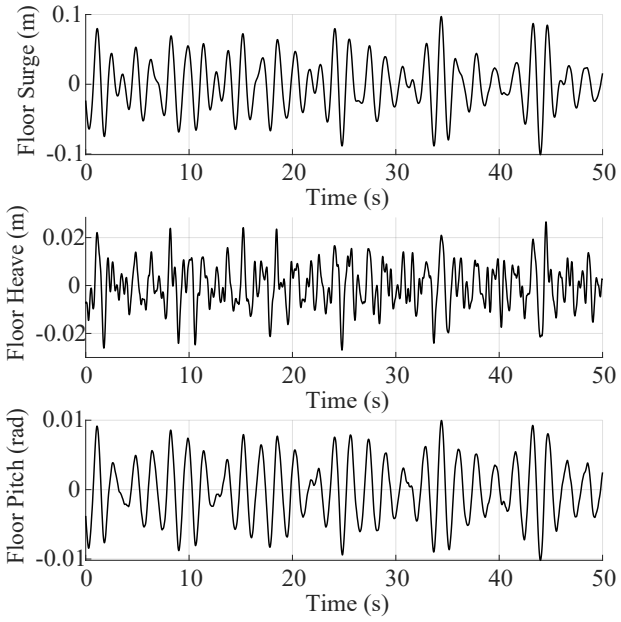

Figure 2. Floor motion in *x*, *z*, and θ directions.

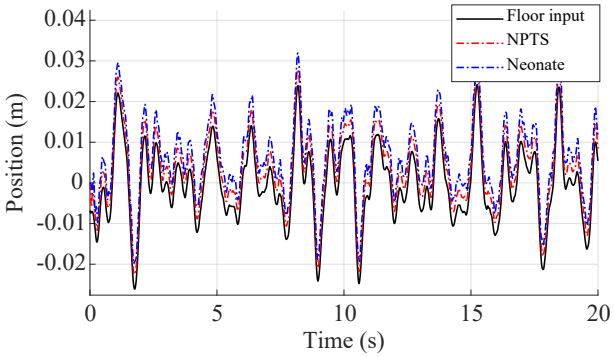

Figure 3. Simulated vertical displacement of NPTS and neonate.

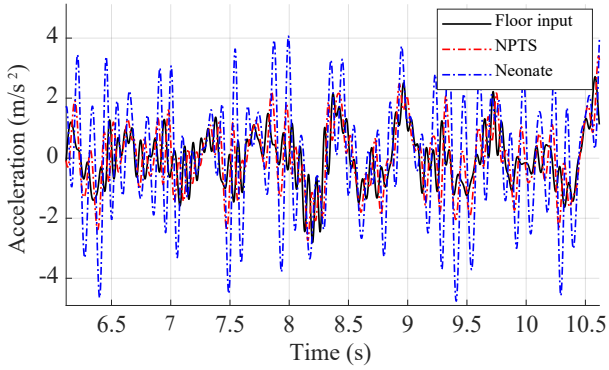

Figure 4. Simulated vertical acceleration of NPTS and neonate.

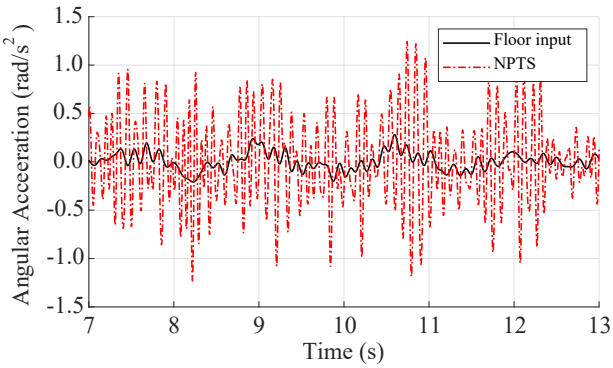

Figure 5. Simulated angular acceleration of NPTS in pitch direction.

TABLE III. STIFFNESS AND DAMPING COEFFICIENTS

Spring – Damper	*Stiffness Coefficient*	*Stiffness Value*	*Damping Coefficient*	*Damping Value*
1	K_1	420000 N/m	C_1	1700 Ns/m
2	K_2	240000 N/m	C_2	1700 Ns/m
3	k	8000 N/m	c	60 Ns/m

The curves corresponding to each body's vertical acceleration, Figs. 6 and 8, exhibit peak magnitudes close to the same frequencies at which the road data peaks, around 2 Hz and 9 Hz. The increase in amplitude between the neonate and NPTS suggests the model's natural frequency around 9 Hz is contributing to this amplification. The angular PSD in Fig. 7 has peaks that are lower than those in the recorded measurements, with the low frequency peak shifted approximately 1 Hz.

These initial results indicate that the derived equations of motion provide the foundation of a viable model of the NPTS, as the vertical frequency response of the NPTS and neonate were closely replicated. Future development will consider additional torsional forces based off the stretcher mounting mechanism, which may improve the angular PSD. As only a single road condition was considered for this simulation, the stiffness and damping parameters will be further optimized to satisfy the PSD of different transport environments in ground and air ambulances, in both pitch and roll directions.

VI. CONCLUSION

The NPTS and stretcher system has been abstracted into a planar model, and the preliminary results of the simulation are indicating this model is representative of the physical system.

The frequency response of this planar model has been simulated by using the Lagrange energy method to determine the equations of motion. The input floor motion was generated using the PSD from a ground ambulance road test, and the output motion of the NPTS centre of mass and patient were found. The model was compared against data recorded during on-road testing, but would benefit from further refinement by tuning parameters to satisfy a variety of transport conditions. The results showed that the power spectral densities in the vertical direction closely match in terms of the frequencies experiencing high magnitude; however, the angular direction exhibits a shift in frequency for one mode and lower amplitudes in both.

Planned work on this model includes solving for the equations of motion in the roll plane and further optimizing the unknown spring-damper parameters. These two models will be tested using various road conditions and discrete event inputs to further improve its response. Ultimately, a three-dimensional model will be constructed that can provide frequency response data at multiple locations across the NPTS in all six degrees of freedom. This model will be used to simulate road and flight environments, and ultimately contribute to the reduction of vibration amplification to increase safety for neonates in transit.

ACKNOWLEDGMENT

We acknowledge the joint support of the Natural Sciences and Engineering Research Council of Canada (NSERC) and the Canadian Institutes of Health Research (CIHR) for this Collaborative Health Research Project [CHRPJ-2020-549669].

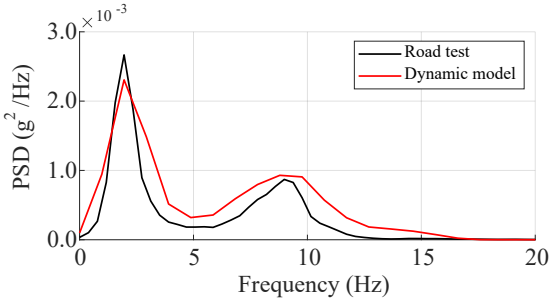

Figure 6. NPTS acceleration PSD in vertical direction.

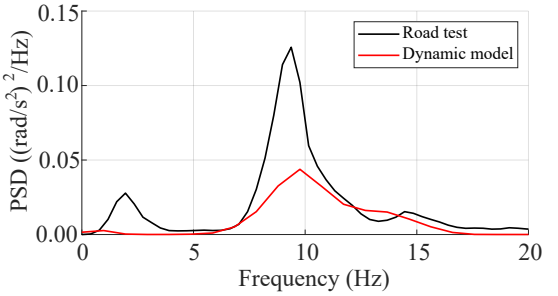

Figure 7. NPTS angular acceleration PSD in pitch direction.

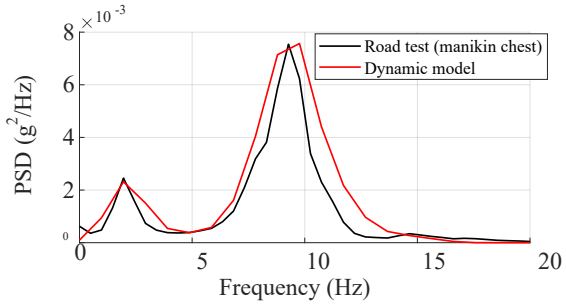

Figure 8. Neonate acceleration PSD in vertical direction.

REFERENCES

[1] M. Ramirez, N. Virdi, K. Greenwood, and R. Zhang, "A provincial neonatal transport incubator for Ontario," in Proceedings of the 37th Canadian Medical and Biological Engineering Conference, 2014.

[2] "Mechanical vibration and shock: Evaluation of human exposure to whole-body vibration: Part 1 General requirements," ISO2631-1, International Organization for Standardization, 1997.

[3] M. Yang, et al., "The dynamic performance optimization for nonlinear vibration-reduction system of the tracked ambulance," Journal of Mechanical Engineering Science, vol. 229, pp. 2715-2719, 2015.

[4] F. Malvezzi, R. M. M. Orsino, K. D. Stavropoulos, "Parameter optimization for a vibration attenuation system on ambulance stretchers," in Vibroengineering Procedia, vol. 37, 2021.

[5] H. C. Chae and S-B Choi, "A new vibration isolation bed stage with magnetorheological dampers for ambulance vehicles," in Smart Materials and Structures, 2015.

[6] M. Bailey-Van Kuren and A. Shukla, "System design for isolation of a neonatal transport unit using passive and semi-active control strategies," Journal of Sound and Vibration, vol. 286, pp. 382-394, 2005.

[7] F. Darwaish et al., "Preliminary laboratory vibration testing of a complete neonatal patient transport system," in Proceedings of the Annual International Conference of the IEEE Engineering in Medicine and Biology Society (EMBS), 2020, vol. 2020-July pp. 6086-6089.

[8] *Vehicle Dynamics Terminology*. SAE J670. Society of Automotive Engineers, Warrendale, PA, 2008.

[9] "Power-PRO™ XT Stryker Operations/Maintenance Manual Rev. C," Stryker Medical, Portage, MI, USA, 2012, pp.11.

[10] J. Isenberg, Presentation, "IB action items following the web conference hosted on July 10, 2014," International Biomedical, Aug. 13, 2014.